COBEM 2023 27TH INTERNATIONAL CONGRESS OF MECHANICAL ENGENEERING

ABCM Brazilian Society of Mechanical Sciences and Engineering
27th ABCM International Congress of Mechanical Engineering
December 04-08, 2023, Florianópolis-SC, Brazil

COB-2023-1558
DETERMINATION OF RADIAL GRINDING WHEEL WEAR BY ACOUSTIC EMISSION

Santiago Javier Caraguay
Universidade Federal de Santa Catarina, Campus Reitor João David Ferreira Lima, Florianópolis – SC, 880400-900, Brazil.
Instituto Senai de Inovação em Sistemas de Manufatura e Processamento a Laser, Rua Arno Waldemar Dohler, Joinville – SC, 89219-510, Brazil
santiago.caraguay@posgrad.ufsc.br

Christian Andrés Caraguay
Universidad Nacional de Loja, Facultad de la Energía, las Industrias y los Recursos Naturales no Renovables, Ciudad Universitaria Guillermo Falconí, Loja, Ecuador
christian.caraguay@unl.edu.ec

Adriano Boaron
Fernando Moreira Bordin
Fabio Antônio Xavier
Universidade Federal de Santa Catarina, Campus Reitor João David Ferreira Lima, Florianópolis – SC, 880400-900, Brazil
aboaron@yahoo.com.br, f.m.bordin@posgrad.ufsc.br, f.xavier@ufsc.com

Abstract. *Grinding is a widely used process in metalworking and other industries, where the quality of the finished product is highly dependent on the grinding wheel's condition. Monitoring the condition of the grinding wheel is, therefore, crucial to ensure dimensional accuracy, quality and to reduce manufacturing costs. Acoustic emission (AE) sensors can provide real-time monitoring of the grinding wheel condition by detecting the acoustic emission signals generated during the grinding process. In this study, a methodology to measure the radial grinding wheel wear through AE sensor is presented and compared with the traditional imprint method. An experimental rig allows to measure the radial grinding wheel wear through an AE-based contact recognition procedure. The coordinates of the grinding tool periphery are saved on the numerical command of the grinding machine, and then compared with the effective width of the grinding wheel after grinding experiments. The radial wear was then calculated by the difference between the saved coordinates. Results showed a good correlation with the AE method and the imprint method. The proposed monitoring method can provide real-time feedback on the grinding wheel's condition, enabling manufacturers to make informed decisions and optimize their operations.*

Keywords: *Acoustic Emission, Grinding wheel wear, Process monitoring, Dimensional accuracy, Grinding.*

1. INTRODUCTION

The grinding process is typically the final finishing process for precision mechanical components in a wide range of industries. This process must ensure high surface quality of the machined components, along with increased process efficiency (Badger, 2012). The growing demands for quality in manufactured components, as well as the increasing requirements for cost and time efficiency, call for enhanced safety and control in the grinding process. As a result, there is a constant need for the implementation of monitoring and control systems to achieve satisfactory results, even under critical conditions (Teti *et al.* 2010).

External plunge cylindrical grinding refers to the grinding of the external surface of a cylindrical workpiece, perpendicular to its axis of rotation. The workpiece is secured either on a clamp or between centers. With the workpiece rotating, material removal begins when the abrasive tool radially plunges against the workpiece, as schematically shown in Figure 1 (Klocke, 2009).

Among the characteristic cutting motions of the process, the following are the most important: the peripheral speed of the grinding wheel (v_s), the peripheral speed of the workpiece (v_w), and the radial infeed velocity of the grinding wheel (v_{fr}). The interaction between v_w and v_{fr} defines the material removal rate Q_w, along with the depth of cut (a_e) on the workpiece surface (Rowe, 2004). Figure 1 also illustrates the grinding width (a_p), the wheel width (b_s), the wheel diameter (d_s), and the workpiece diameter (d_w).

One of the key parameters in the grinding process is the material removal rate (Q_w), which represents the volume of material removed from the workpiece (V_w) per unit of time. The specific material removal rate (Q'_w) allows for the

comparison of material removal between equivalent processes, irrespective of the effective grinding width. In external plunge cylindrical grinding, the specific material removal rate is calculated using Equation 1 (Klocke, 2009).

$$Q'_w = \pi . d_w . v_{fr}, \quad (1)$$

where, d_w is the workpiece diameter (mm) and v_{fr} = radial infeed velocity ($mm.s^{-1}$).

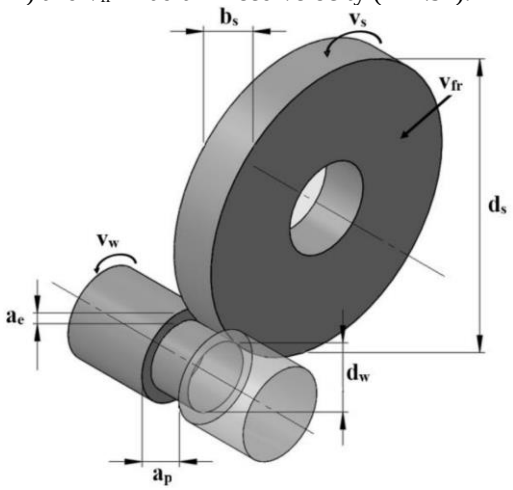

Figure 1. Schematic diagram of External plunge cylindrical grinding.

When a grinding wheel presents excessive wear, several problems can arise. The grinding wheel cutting efficiency decreases, resulting in slower material removal rates and reduced productivity. Also, increased wear leads to loss of wheel shape and integrity, causing surface irregularities, vibrations, and chatter marks on the workpiece (Couey, 2005). Moreover, excessive wheel wear may result in thermal damage due to elevated temperatures, compromising the material properties of the workpiece (Tönshoff, 2002). Consequently, effective control and measurement of grinding wheel wear are essential to avoid these detrimental effects.

The macrotopography of the grinding wheel is considered one of the most important aspects of the process, as it directly influences the dimensional accuracy of the ground workpiece. The geometry of the workpiece is not only influenced by the dimensional precision and macrogeometric wear of the grinding wheel but also by the vibrations generated during the process and the accuracy of machine alignments and movements (Rowe, 2004). Accurately measuring radial grinding wheel wear is crucial for evaluating the condition and effectiveness of the grinding process. Several methodologies have been developed for this purpose, with imprint methods being widely used in industry. These methods involve replicating the wheel profile onto a counterbody, typically made of carbon, to assess the amount of wear on the wheel. However, it is important to ensure the accuracy of this determination, as any inaccuracies can lead to compromised part dimensions and potentially require rework.

Monitoring and controlling grinding wheel wear are essential for maintaining process efficiency, workpiece quality, and cost-effectiveness (Byrne, 1995). Real-time monitoring of grinding wheel wear offers numerous advantages. Continuous monitoring allows for timely detection of wear progression, facilitating proactive maintenance and minimizing unexpected machine downtime. It also provides valuable data for process optimization, allowing adjustments to be made to parameters such as feed rate, coolant application, and wheel dressing. By monitoring wear, operators can ensure the grinding process remains within desired quality limits and achieve longer wheel lifespan, reduced costs, and improved workpiece quality.

Acoustic emission (AE) has emerged as a promising technique for monitoring small magnitudes of grinding wheel wear (Caraguay, 2022). AE involves the detection and analysis of high-frequency stress waves generated by material deformation or damage. Due to the small magnitudes of wear in grinding operations, AE offers high sensitivity and accuracy in detecting subtle changes in the grinding wheel condition. By integrating AE sensors into the grinding machine, the wear progression can be monitored in real-time, allowing for timely intervention and maintenance actions.

In this context, this article aims to measure the radial grinding wheel wear through acoustic emission. An AE monitoring system was integrated with the CNC of the grinding machine as previously proposed and developed by (Boaron 2009), (Weingaertner, 2012). This method based on AE allowed for precise contact recognition between the grinding wheel and the diamond tip within the elastic deformation range (Boaron, 2015), (Boaron, 2018). An AE recognition procedure was applied to obtain a reference position between the grinding wheel periphery and the diamond tip during the initial contact (Boaron, 2015). The monitoring system automatically triggered the numerical command (NC) of the grinding machine, allowing for the determination of the radial wear. The methodology was validated through comparison with the imprint method.

2. MATERIALS AND METHODS

2.1 Experimental rig and monitoring system

Figure 2 schematically presents the experimental setup used for the external plunge cylindrical grinding tests and for radial grinding wheel wear determination. The tests were performed on a CNC universal cylindrical grinder, Pratika Flexa 600L model, manufactured by Zema Zselics Ltda.

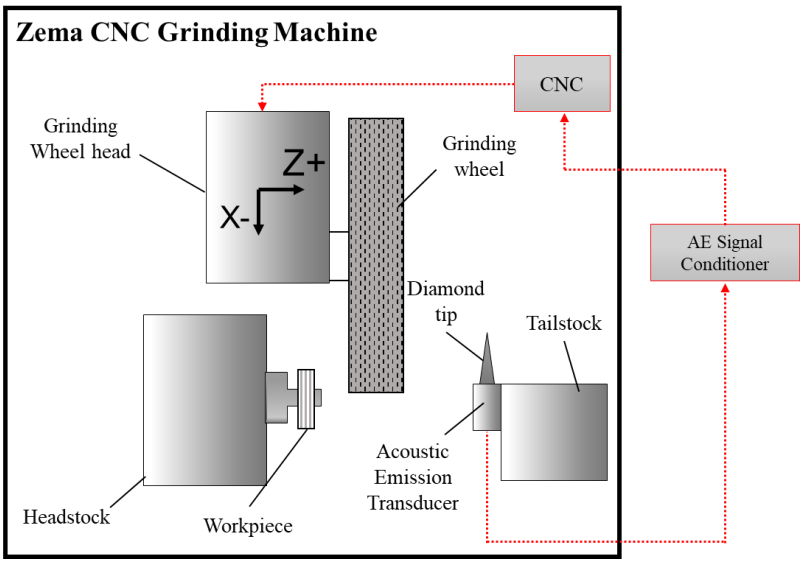

Figure 2. Schematic diagram of experimental setup. [Adapted and based on (Boaron, 2009), (Weingaertner, 2012) and (Boaron, 2015)].

In order to evaluate the wear of the radial grinding wheel, a monitoring system using acoustic emission was integrated into the CNC command of the grinding machine (Boaron, 2009), (Weingaertner, 2012). A diamond tip dresser was securely attached to the tailstock of the grinding machine, while an AE transducer was fixed onto the support of the diamond tip (Boaron, 2015), (Boaron, 2018). By employing this instrumented method based on AE, it became possible to recognize the contact between the grinding wheel and the diamond tip with precision within a range of a few micrometers, which falls within the elastic deformation range of the diamond(Weingaertner, 2012), (Boaron, 2015), (Boaron, 2018).

The CNC command of the grinding machine stores the machine coordinates (X and Z) associated with the initial contact between the grinding wheel and the diamond tip (Boaron, 2009), (Boaron, 2015). The dotted lines represent the flow of signals in the contact recognition process. As the interference between the grinding wheel and the diamond tip measures less than 1 µm, signifying an elastic contact between the abrasive grains of the grinding wheel and the diamond tip, any damage to the abrasive grains and wear of the diamond tip can be neglected (Weingaertner, 2012), (Boaron, 2009), (Boaron, 2015), (Boaron, 2018).

The grinding wheel employed in the process was a vitrified bonded wheel made of Al_2O_3 (A80 J 6 V). This specification indicates that the wheel consisted of aluminum oxide abrasive grains with an average grain size of FEPA 80, equivalent to 185 µm. It had a hardness rating of J, a porosity level of 6, and was bonded with a vitreous material (V). The grinding wheel had an external diameter of 400 mm, an internal diameter of 203 mm, and a width of 30 mm. Further details regarding the dimensions, composition, and parameters for the dressing process can be found in Table 1.

Table 1. Composition of the grinding wheel and dressing process parameters.

Dressing Process parameters	**Grinding wheel**	**Dressing Tool**
v_{sd}: 30 m/s	Fused Aluminum oxide	Multi-grit Diamond
v_{fa}: 1432 mm/s	High purity alumina > 99 %	b_d: 4 mm
U_d: 4	A80 J 6 V 50	Oil-based coolant: 3%
a_{ed}: 10 µm	External diameter: 400 mm	water concentration
	Internal diameter: 203 mm	
	Width: 30 mm	

During the dressing procedure, a multi-grit diamond dressing tool with a dressing width of bd = 4 mm was utilized. The grinding wheel's peripheral speed while dressing was vsd = 30 m/s, and a dressing overlap ratio of Ud = 4 was chosen. The depth of the dressing cut was established at aed = 10 μm. As the dressing took place, the grinding wheel moved along the dressing tool at an axial dressing feed rate of vfad = 1432 mm/s.

2.2 Grinding experiments

The purpose of the grinding experiments was to intentionally induce wear on the grinding wheel to validate the radial wheel wear procedure with Acoustic Emission, and also, to measure the radial grinding wheel wear for different specific material removal rates. The experiments consisted in external plunge cylindrical grinding of nodular cast iron GGG70, utilizing electro-fused Al_2O_3 grinding wheels. The specific material removal rate of 6, 8, 10 and 14 200 mm^3/mm.s was employed, to remove a specific material removal of V'_w = 200 mm^3/mm. The material removal rate was determining using the equation 1. Also, for the material removal rate of Q´w= 6 mm^3/mm.s, the wear was measured for a total V'_w = 800 mm^3/mm, achieved with increments of V'_w = 200 mm^3/mm. The grinding process was carried out in a single cycle, without employing a spark-out phase. Table 2 presents the machining parameters employed.

Table 2. Grinding experiments parameters.

Grinding process	Workpiece Material
External cylindrical plunge grinding	Nodular Cast Iron
v_s= 30 m/s	(GGG 70)
n= 4	Hardness: 290 HB
n_s= 1432 rpm	d_w: 62 mm
n_w= 350 rpm	b_w: 10 mm
L_{eff}= 10 mm	Oil-based coolant: 3%
Q'_w= 6, 8, 10 and 14 mm^3/mm.s	water concentration
V'_w= 200 mm^3/mm	
Q'_w= 6 mm^3/mm.s;	
V'_w= 200, 400, 600 and 800 mm^3/mm	

Throughout the process, the rotational ratio between the grinding wheel and the workpiece remained constant. Prior to each test, the grinding wheel underwent dressing in order to assess the impact of the specific material removal rate on the grinding wheel wear. The tests were conducted using a 10 mm effective width of the grinding wheel (L_{eff}). The specific material removal rates used are for roughing grinding. After the tests, the grinding wheel wear was measured.

2.3 Validation of radial grinding wheel wear by AE

In order to validate the accuracy of the SM/EA method in determining the radial wear of the grinding wheel, the obtained values of radial wear through the profile imprint method on a reference workpiece (RW) were compared with the numerical values acquired via the integration of SM/EA in the CNC command of the machine tool, following the methodology outlined by (Weingaertner, 2012), (Boaron, 2009). For this validation, a V'_w: 800 mm3/mm was removed using a Q'_w: 6 mm^3/mm.s.

Figure 3 illustrates the dimensions of the RW that was manufactured using nodular cast iron GGG 70. The RW was designed with a width of 20 mm to accurately imprint the effective width of the grinding wheel (L_{eff}) and establish reference regions for assessing radial wear. To facilitate the attachment of the nut with the support fixture, an internal turning operation was conducted, resulting in a recessed hole with a diameter of 40 mm and a depth of 10 mm.

The profile imprint method was employed to indirectly determine the radial wear of the grinding wheel. This method involves examining the replicated profile of the grinding wheel on the RW. The profile obtained is directly related to the radial grinding wheel wear (Δrs) at the effective width of the grinding wheel. The profile imprint on the reference workpiece was achieved by conducting external plunge cylindrical grinding, utilizing a specific grinding rate of Q'w = 0.6 mm^3/mm.s. A lower rate was chosen to prevent excessive wear of the grinding wheel. The plunge depth of the wheel was carefully controlled to ensure that the entire width of the grinding wheel profile was imprinted on the RW.

For evaluating the replicated profile on the RW, a Form Talysurf i-120 profilometer from Taylor Hobson® was utilized. An inductive probe with a diamond tip radius of 2 μm was employed for the measurements. The ULTRA software, which controls the profilometer, was used to perform the profile measurements. This software not only facilitates the measurement process but also stores the acquired profiles, enabling the calculation of radial wear values.

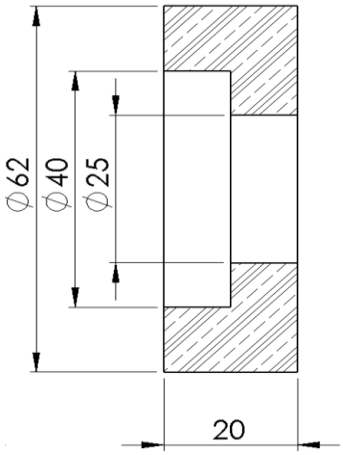

Figure 3. Reference workpiece used to indirectly measure the grinding wheel wear by the imprint method.

The procedure for determining the replicated grinding wheel profile on the RW involved the linear movement of the inductive probe in contact with the RW surface. Measurements were taken with a transverse evaluation length of 13 mm, following the direction width of the RW. Three equidistant measurements were conducted along the RW's periphery. The collected profiles were analyzed using the Talyprofile software and the grinding wheel wear was determined.

To assess the radial grinding wheel wear, the AE monitoring system was integrated into the CNC of the grinding machine (Boaron, 2009), (Weingaertner, 2012). To obtain a reference position between the grinding wheel periphery and the diamond tip when the first contact is detected, a validated AE recognition procedure was applied (Boaron, 2009), (Weingaertner, 2012), (Boaron, 2015), (Boaron, 2018). Figure 4 provides a schematic representation of the evaluation of radial grinding wheel wear (Δ_{rs}) using the AE contact recognition procedure. The procedure begins with the grinding wheel positioned 0.5 mm away from the diamond tip, while rotating at a peripheral speed of v_s = 30 m/s (Figure 4.a1). The tool moves towards the diamond tip with a radial infeed velocity of v_{fr1} = 0.5 mm/min until the AE transducer detects the first contact (Figure 4.a2).

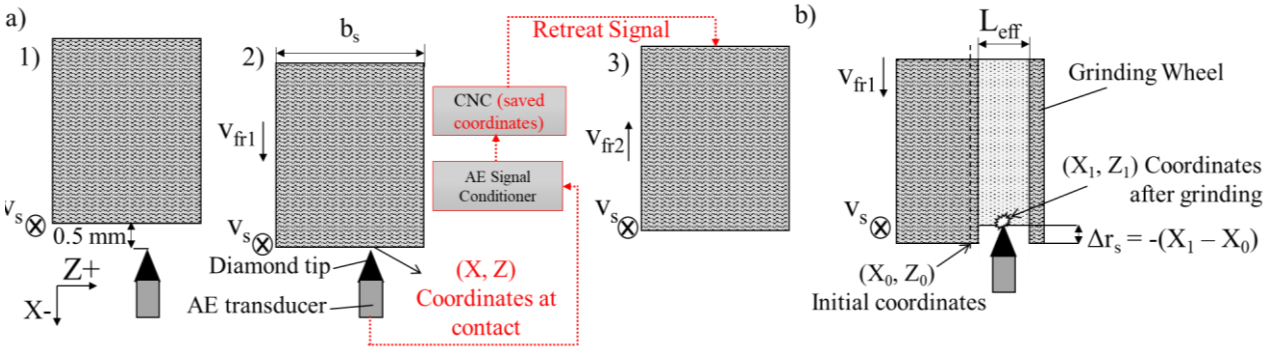

Figure 4. Grinding wheel radial wear determination through Acoustic Emission: a) contact recognition procedure and b) determination of radial grinding wheel wear.

Upon contact, the monitoring system automatically sends a signal to the numerical command (NC) of the grinding machine, resulting in the retreat of the grinding wheel at a velocity of v_{fr2} = 6000 mm/min (Figure 4.a3). The coordinates are stored on the CNC grinding machine for further analysis. Eleven contact recognitions were performed at the same wheel point to determine the system's repeatability. After conducting the contacts, a measurement repeatability of ± 0.75 µm was obtained for the system, with a significance level of α = 0.05.

The process for determining the radial wear values of the grinding wheel is illustrated in Figure 4b. The initial coordinates (X0, Z0) acquired during the contact recognition procedure correspond to the tool periphery where no grinding took place. The Z0 coordinate is located at the center of the grinding wheel's width. The grinding experiments are conducted across the effective width of the grinding wheel (L_{eff}). Following the material removal, the contact recognition procedure is executed, resulting in the acquisition of contact coordinates (X1, Z1). These coordinates correspond to the tool periphery along the L_{eff} after the completion of the grinding experiment. The radial wheel wear value (Δrs) is determined by subtracting the initial X0 coordinate from the X1 coordinate. To obtain an average value for the radial wheel wear, three equidistant contact measurements are performed along the L_{eff}.

3. RESULTS

3.1 Validation of radial grinding wheel wear by AE

The profile imprint method was employed to indirectly determine the radial wear of the grinding wheel. This method involves examining the replicated profile of the grinding wheel on the RW. The profile obtained is directly related to the radial grinding wheel wear (Δ_{rs}) at the effective width of the grinding wheel. Figure 5 shows the imprint method and the corresponding measured profile with a profilometer.

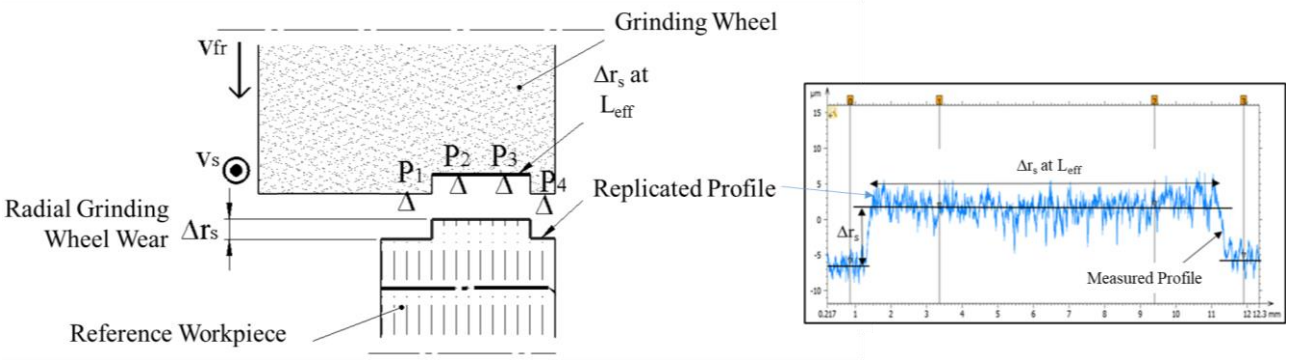

Figure 5. Results of the imprint method to measure the radial grinding wheel wear.

Figure 5 also displays the worn profile of the grinding wheel, indirectly obtained through the measurement of the replicated profile on the RW. The distances between (0-1) and (2-3) correspond to the approximate distances between points (P1-P2) and (P3-P4), respectively. The determination of radial wear involved calculating the difference between the average profile along the grinding region and the average profile of the reference regions on the replicated profile. The values from all measurements were computed to determine the average wear value of the measured profile. The average radial wear obtained using the profile imprint method was Δ_{rs} = (7.5 ± 2) µm.

To evaluate the grinding wheel wear using acoustic emission (AE), the contact recognition procedure described in Section 2.3 was carried out. The contact recognition measurements were conducted at approximately four specific points (P1, P2, P3, P4) as illustrated in Figure 5. These measurements were taken both before and after performing the external plunge cylindrical grinding tests. The resulting values of radial grinding wheel wear (Δ_{rs}) obtained from the contact recognition process are presented in Table 3.

Table 3 – Radial grinding wheel wear results for 6 mm^3/mm.s and V'$_w$: 800 mm^3/mm conditions .

	Dressed grinding wheel (mm)	**Grinding wheel after experiments (mm)**	**Radial grinding wheel wear (µm)**
Point P$_1$	46,128	46,127	0,5
Point P$_2$	46,124	46,111	6,5
Point P$_3$	46,130	46,115	7,5
Point P$_4$	46,132	46,130	1

After the contact recognition at each point, the parameter R149 of the CNC machine tool corresponds to the actual diameter of the grinding wheel position with the diamond tip, relative to a reference diameter ($Ø_{ref}$ = 42.6 mm). This diameter serves as a reference for the position of the grinding wheel in relation to the diamond tip before performing the contact recognition. The presented values correspond to the wear obtained after machining a V'w = 800 mm3/mm with Q'w = 6 mm^3/mm.s.

The radial wear of the grinding wheel is determined by comparing the diameters before and after the grinding experiments. The results indicate that the P1 and P4 measurements show minimal changes, while P2 and P3 exhibit significant differences. As P2 and P3 were measured at the L_{eff} (effective width of the grinding wheel), it is expected that the relative position between the grinding wheel and the diamond tip, which corresponds to the grinding wheel wear after

machining, would undergo more noticeable changes. The resulting values are then divided by two, resulting in a radial wear of (7 ± 0.75) µm.

The correlation between the average values of radial wear using different methods (AE and imprint method) allows for the application of the contact recognition procedure to assess radial wear during the conducted tests in this research.

3.2 Radial grinding wheel wear after grinding experiments

To compare the macro-topographic changes in the grinding wheel, measurements of grinding wheel radial wear were conducted. Figure 6.a illustrates the results of grinding wheel radial wear for different V'_w values, specifically focusing on Q'_w = 6 mm^3/mm.s. The findings indicate that the grinding wheel exhibited an initial pronounced radial wear rate (V'_w = 0-200 mm^3/mm) immediately after dressing, followed by a stable and consistent wear rate (V'_w = 200 - 600 mm^3/mm). The initial higher wear rate of the grinding wheel can be attributed to the breakout of abrasive grains, which occurs due to structural damage or excessive protrusion of the grains after dressing. This phenomenon leads to early abrasive fracture (Feng, 2009). As the grinding process progresses, the wear rate stabilizes, primarily driven by the micro-wear mechanism.

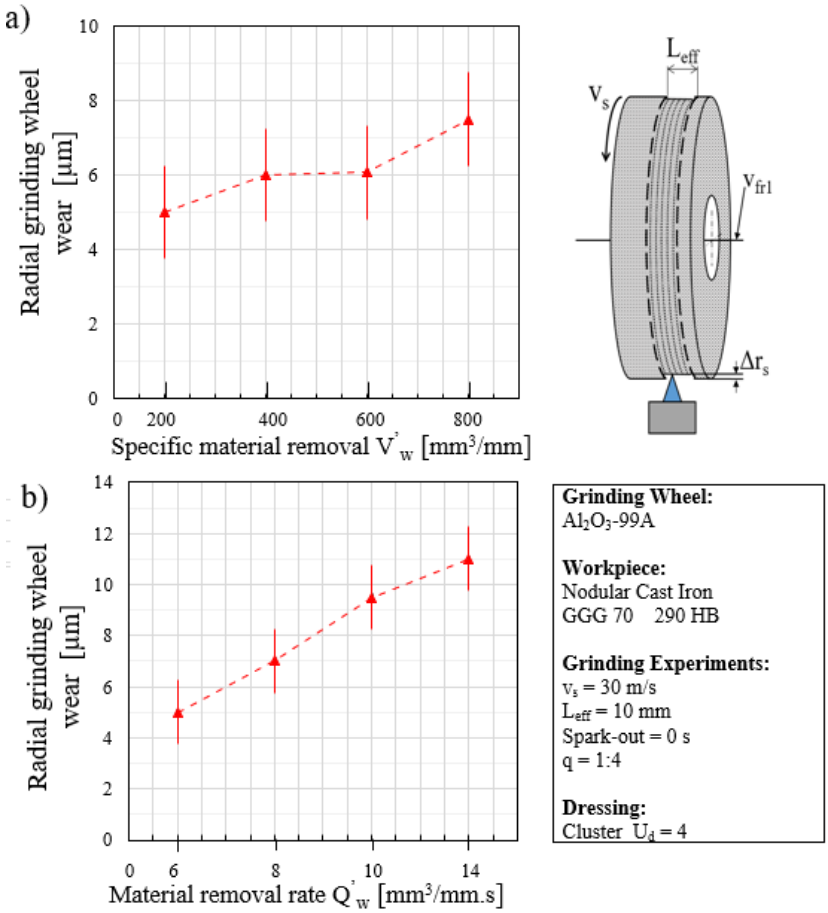

Figure 6. Results of the radial grinding wheel wear as a function of a) specific material removal (V´w) and b) specific material removal rate (Q´w).

Figure 6.b shows the results of the grinding wheel radial wear for different Q'_w values after removing a V'_w = 200 mm^3/mm. The findings indicate that specific material removal rate has a significant impact in the radial grinding wheel wear, showing an increased value as the Q'_w increases. The grinding wheel radial wear increases for higher material removal rates due to the increased contact and friction between the abrasive grains on the wheel and the workpiece material. As the material removal rate increases, more abrasive grains come into contact with the workpiece surface, resulting in greater wear on the grinding wheel. The increased contact and friction can generate higher temperatures and stresses, leading to accelerated wear of the abrasive grains and the bond material that holds them together. Additionally, the higher material removal rates can cause more aggressive cutting action, further contributing to the wear of the grinding wheel. Therefore, it is expected that as the material removal rate increases, the grinding wheel experiences greater radial wear.

4. CONCLUSION

This article presented an in-depth exploration of the measurement and monitoring of radial grinding wheel wear using acoustic emission (AE). The experimental setup, methodology, and results were discussed in detail. The integration of AE monitoring into the CNC grinding machine allowed for precise contact recognition and evaluation of small magnitudes of grinding wheel wear. The radial wear of the grinding wheel was determined using both the profile imprint method and the contact recognition procedure with AE. The profile imprint method provided valuable insights into the macro-topographic changes of the grinding wheel, while the contact recognition procedure allowed for the assessment of radial wear at specific points.

Comparing the results from both methods, there was a correlation between the average values of radial wear, confirming the reliability and applicability of the contact recognition procedure. This method allows for real-time monitoring of the grinding wheel wear during the experiments. The results, also revealed that the grinding wheel exhibited an initial pronounced wear rate immediately after dressing, followed by a stable and consistent wear rate during the grinding process.

Furthermore, the results highlighted the influence of the specific material removal rate (Q'w) on the radial wear of the grinding wheel. As the material removal rate increased, the wear rate of the grinding wheel also increased which can be attributed to the intensified contact and friction between the abrasive grains and the workpiece material, resulting in accelerated wear of the grinding wheel.

Overall, the ability to accurately measure and monitor the radial wear of the grinding wheel is crucial for ensuring optimal grinding performance and quality. The findings of this study contribute to a better understanding of the wear behavior and provide insights for the optimization of grinding processes and wheel selection in various industrial applications. The monitoring system can be used to optimize the grinding process, minimizing downtime, and avoiding excessive wear that could compromise the workpiece quality. AE offers a reliable and sensitive method for detecting and quantifying small magnitudes of grinding wheel wear. By integrating AE monitoring into the CNC command, real-time data on wheel wear can be obtained, allowing for proactive maintenance and process adjustments.

5. ACKNOWLEDGEMENTS

The authors gratefully acknowledge Conselho Nacional de Desenvolvimento Científico e Tecnológico (CNPq) and Coordenação de Aperfeiçoamento de Pessoal de Nível Superior (CAPES) for the assistance provided for the development of this work.

6. REFERENCES

Badger, J., 2012. Microfracturing Ceramic Abrasive in Grinding. *International Manufacturing Science and Engineering Conference*.

Boaron, A. 2009. *Determinação do posicionamento relativo entre rebolo e peça com o auxílio da emissão acústica (in Portuguese)*. Master Science Dissertation, Graduate Program in Mechanical Engineering, Federal University of Santa Catarina, Florianópolis, Brasil.

Boaron, A. 2015. *Desenvolvimento e validação de um método dinâmico, baseado em EA, para a caracterização em processo de rebolos convencionais (in Portuguese)*. Ph.D. thesis, Graduate Program in Mechanical Engineering, Federal University of Santa Catarina, Florianópolis, Brasil.

Boaron, A., Weingaertner, W. L. 2018. Dynamic in-process characterization method based on acoustic emission for topographic assessment of conventional grinding wheels. Wear: An International Journal on the Science and Technology of Friction, Lubrication. Vol. 406-407, pp. 218-229.

Byrne, G., Dornfeld, D., Inasaki, I., Ketteler G., König, W., Teti, R., 1995. Tool Condition Monitoring (TCM) The Status of Research and Industrial Application. In CIRP Annals, Vol. 44, pp. 541–567.

Caraguay, S.J., Boaron, A., Weingaertner, W.L., Bordin, F.M., Xavier, F.A. 2022. Wear assessment of microcrystalline and electrofused aluminum oxide grinding wheels by multi-sensor monitoring technique. Journal of manufacturing processes, Vol. 80, pp. 141-151.

Couey, J.A., Marsh, E.R., Knapp, B.R., and Vallance R.R., 2005. Monitoring force in precision cylindrical grinding. Precision Engineering, Vol. 29, pp. 307–314.

Feng, J., Kim. B.S., Shih, A. and Ni, J. 2009. Tool wear monitoring for micro-end grinding of ceramic materials. Journal of Materials Processing Technology, Vol. 209, pp. 5110–5116.

Klocke, F., 2009. *Manufacturing processes 2: Grinding, Honing, Lapping*. Berlin.

Rowe W., Marinescu I. D., 2004. *Tribology of abrasive machining processes.* Norwich.

Teti, R., Jemielniak, K., O'donnell, G., Dornfeld, D., 2010. Advanced monitoring of machining operations. CIRP Annals, Vol. 59, pp. 717–739.

Tönshoff, H. K., Friemuth, T., Becker, J. C., 2002. Process Monitoring in Grinding. In CIRP Annals, Vol. 51, pp. 551–571.

Weingaertner, W.L., Boaron, A.,2012 Determination of the relative position between grinding wheel and a cylindrical workpiece on a 7 axis grinding machine by acoustic emission. Journal of the Brazilian Society of Mechanical Science and Engineering. Vol. 34, pp. 24–31.

7. RESPONSIBILITY NOTICE

The authors are the only responsible for the printed material included in this paper.